Predicting community dynamics of antibiotic sensitive and resistant species in fluctuating environments

Olga A. Nev*, Alys Jepson*, Robert E. Beardmore, and Ivana Gudelj**

* these authors contributed equally; Olga Nev, Biosciences and Living Systems Institute, University of Exeter, Exeter EX4 4QD, UK; o.nev@exeter.ac.uk; Alys Jepson, Biosciences and Living Systems Institute, University of Exeter, Exeter EX4 4QD, UK; a.k.jepson@exeter.ac.uk

** corresponding author; Ivana Gudelj, Biosciences and Living Systems Institute, University of Exeter, Exeter EX4 4QD, UK; i.gudelj@exeter.ac.uk; tel: +44 (0) 1392 725840; fax: +44 (0)1392 263434

Robert E. Beardmore, Biosciences and Living Systems Institute, University of Exeter, Exeter EX4 4QD, UK; r.e.beardmore@exeter.ac.uk

Key words: antimicrobial resistance, environmental fluctuations, multi-species communities, coexistence, mathematical models

Abstract

Microbes occupy almost every niche within and on their human hosts. Whether colonising the gut, mouth or bloodstream, micro-organisms face temporal fluctuations in resources and stressors within their niche but we still know little of how environmental fluctuations mediate certain microbial phenotypes, notably antimicrobial resistant ones. For instance, do rapid or slow fluctuations in nutrient and antimicrobial concentrations select for, or against, resistance?

We tackle this question using an ecological approach by studying the dynamics of a synthetic and pathogenic microbial community containing two species, one sensitive and the other resistant to an antibiotic drug where the community is exposed to different rates of environmental fluctuation. We provide mathematical models, supported by experimental data, to demonstrate that simple community outcomes, like competitive exclusion, can shift to coexistence and ecosystem bistability as fluctuation rates vary. Theory gives mechanistic insight into how these dynamical regimes are related.

Importantly, our approach highlights a fundamental difference between resistance in single species populations, the context in which it is usually assayed, and in communities. While fast environmental changes are known to select against resistance in single-species populations, here we show that they can promote the resistant species in mixed-species communities. Our theoretical observations are verified empirically using a two-species *Candida community.*

1 Introduction

Microbes live in complex and diverse communities colonising almost every niche within and on the human body [1]. The gut, vagina and skin are known to contain diverse microbial communities that differ remarkably between host individuals [1]. We are also beginning to discover that microbes occupy sites thought previously to be sterile, such as the womb [2].

The composition of microbial communities is affected by resources [3, 4, 5] and drugs [6], both of which are subject to temporal fluctuations. For example, nutrient availability in the form of glucose concentration is known to vary in urine [7], gut [8] and blood with substantial daily variations [9, 10]. In addition, clinicians vary drug dosing regiments [11, 12, 13] which can lead to fluctuations in drug concentrations within a host niche. Moreover, daily drug fluctuations can also arise when the majority of an administered drug is recovered unchanged in a patient's urine within 24 hours after administration of a single dose [12, 14].

How do environmental fluctuations in resources and drug concentrations mediate drug-resistance within a microbial community? It is increasingly recognised that antimicrobial resistance is an ecological as well as a genetic problem [15, 16, 17] with sensitive and resistant species competing for limited nutrients. While the expectation is that resistant species have a competitive advantage over sensitive ones in the presence of a drug, empirical observations demonstrate that they can coexist [18, 19, 20]. What isn't known is how this coexistence as well as other possible competitive outcomes are influenced by fluctuating environments.

The limited understanding of microbial response to fluctuating environments comes in the majority from single species studies. The selection for mutations in fluctuating environments has been extensively studied in theory [21, 22, 23, 24, 25] showing that complex interactions between dynamics of the environment and dynamics of adaptation can affect selection. In addition, experimental studies have shown that fluctuating environments have a profound effect on selection for antibiotic resistance [26, 27, 28] suggesting that rapid fluctuations could avoid the evolution of resistance.

In the context of multi-species communities, the focus has mainly been on identifying conditions of species coexistence in fluctuating environments, with some experimental [29] but mainly theoretical considerations [30, 31, 32, 33, 34]. Here we ask a different question, do rapid or slow fluctuations of microbial

nutrients and antimicrobials select for, or against antimicrobial resistance in a multi-species community?

To this end, we develop a model of the simplest possible community of two species, S and R, and assume that the former is sensitive to an antimicrobial while the latter is resistant. The two species compete for a limiting resource in the presence of the antimicrobial drug in a spatially homogeneous environment. After a period of growth a small fraction of the population is transferred into a new environment containing replenished resources and drugs.

The model is parameterised by *Candida albicans* and *Candida glabrata* growth data from [35]. *C. albicans* and *C. glabrata* are members of healthy human microbiota, but in immunocompromised patients can become pathogenic, leading not only to mucosal infections [36], but also life-threatening disseminated infections [37]. Candidiasis is one of the top ten fungal diseases, which in total kill as many people each year as tuberculosis or malaria [38]. Infections are associated with high mortality, especially bloodstream candidiasis (46% to 75% [38, 39, 40]), and are difficult to diagnose. The majority of infections are caused by *C. albicans*, however mixed-species infections with *C. glabrata* are increasing in occurrence [41]. Such mixed-species infections are thought to be more severe and difficult to treat than single species infections due to their dual pathogenic effect and the fact that *C. glabrata* is relatively unresponsive to the most frequently used antifungal drug fluconazole [42, 43, 44].

Our model identifies regions that delineate resource and drug concentrations where competition between resistant and sensitive species gives rise to exclusion, bistability and coexistence. These regions are shaped by the frequency of environmental fluctuations. In particular, we find regions for which a slow rate of environmental change can promote the resistant species. In other regions, we find that the outcome of competition can be independent of the fluctuation frequency. Finally, contrary to previous findings for single species [26, 27], in certain environments, a fast rate of environmental fluctuation can support the prevalence of resistance. We qualitatively verify these predictions using laboratory competitions between *C. albicans* and *C. glabrata*.

Our results highlight a fundamental difference between resistance in single species assays, the context where it is always assayed, and resistance in microbial communities. In the latter, we show both that a drug-susceptible species can be maintained in the presence of drug and that fast environmental changes

that can mitigate resistance in single species studies [26, 27] can inadvertently promote growth of resistant species in mixed-species communities. This is because the competition for fluctuating nutrients between species, and therefore between two differing metabolic strategies, introduces an extra dimension which is not considered in single species studies.

2 Materials and methods

2.1 Mathematical model of multi-species competition

Consider a microbial community consisting of two species, S and R, competing for a limiting nutrient, N. S is assumed to be sensitive to an antimicrobial drug D, while R is resistant to it.

In our model, all cells take up an extracellular nutrient and convert it into adenosine-5$^{'}$-triphosphate (ATP) using a simple unbranched metabolic pathway [45, 46]. The rate of ATP production in the pathway is given by $q_k \times n_{\mathrm{ATP},k}$, where q_k denotes the rate of the pathway while $n_{\mathrm{ATP},k}$ is the number of ATP units produced per one unit of nutrient in the pathway. The subscript k takes the form $k = \mathrm{S}$ or $k = \mathrm{R}$ referring to the sensitive or resistance species, respectively; this is represented mathematically as $k \in \{\mathrm{S},\mathrm{R}\}$.

As in [45, 46] we make a simplifying assumption that the behaviour of the entire pathway can be modelled with Michaelis-Menten kinetics of a single reaction. Thus q_k is the following function of the concentration N of the limiting nutrient:

$$q_k(N) = \frac{V_{\mathrm{max},k} \times N}{K_{\mathrm{m},k} + N} \,, \quad k \in \{\mathrm{S},\mathrm{R}\} \,, \tag{1}$$

with $V_{\mathrm{max},k}$ denoting the maximal rate of the pathway and $K_{\mathrm{m},k}$ representing the Michaelis-Menten constant corresponding to the species $k \in \{\mathrm{S},\mathrm{R}\}$. The pathway rate $q_k(N)$ represents the rate at which the product is formed which in this case is the same as the rate at which the nutrient is consumed. Therefore, throughout this paper we refer to $V_{\mathrm{max},k}$ as the maximal rate of nutrient uptake and $K_{\mathrm{m},k}$ as the measure of affinity for a nutrient corresponding to the species $k \in \{\mathrm{S},\mathrm{R}\}$.

If microbes are limited by their energetic resource, the amount of biomass formed per unit of ATP is approximately constant and does not depend on the model of ATP production [47]. Thus, as highlighted by [48], if the rate of ATP production increases, the rate of biomass formation and thus the growth rate

of an organism increases. Therefore, in our model the growth rate is represented as a linear function of of the rate of ATP production, namely $G_k \times q_k(N) \times n_{\mathrm{ATP},k}$, with G_k denoting a proportionality constant and $k \in \{\mathrm{S},\mathrm{R}\}$.

The influence of the drug is modelled as a reduction in growth as suggested elsewhere [35] and we briefly summarise the assumptions here. First, we assume that drug growth suppression is the accumulation of processes that decrease per capita growth rate in a non-linear and concentration-dependent manner, with greater inhibition at higher drug concentrations. Second, we assume that the inhibitory effect of the drug on growth depends only on the intracellular accumulation of the drug. Therefore, as in [35], we represent reduction in growth by a function $0 \leq i(D_{\mathrm{in,S}}) \leq 1$ which takes the form:

$$i(D_{\mathrm{in,S}}) = 1 - \frac{a \times (D_{\mathrm{in,S}})^c}{b^c + (D_{\mathrm{in,S}})^c}, \tag{2}$$

where $D_{\mathrm{in,S}}$ is the intracellular concentration of the drug in S, measured in pmol/ml. The parameters a, b, and c describe individual properties of S related to its sensitivity to the drug.

In may be instructive to note that the concentration of S cells is *not* incorporated explicitly into the inhibition function $i(D_{\mathrm{in,S}})$ which, as a result, only depends on the quantity of internalised drug per ml and not *drug per cell*. Thus, inhibition due to drug is not measured here per cell but is instead measured per target per ml inside the cell, assuming those drug targets are sufficient in number and sufficiently diffuse inside cells that their concentration (in ml) can be defined and that this is homogeneous throughout the cell.

Since R is resistant to the drug, there is no drug-induced reduction in its growth and hence we set $i(D_{\mathrm{in,R}}) = 1$. For simplicity we do not model the resistance mechanism explicitly. Moreover, we assume no horizontal gene transfer of resistance between the two species.

Third, we assume that drug import is a saturating function of the extracellular drug concentration (D_{ex}) which takes the form:

$$I(D_{\mathrm{ex}}) = \frac{V_{\mathrm{i},k} \times D_{\mathrm{ex}}}{K_{\mathrm{i},k} + D_{\mathrm{ex}}}\,, \quad k \in \{\mathrm{S},\mathrm{R}\}\,, \tag{3}$$

where $V_{\mathrm{i},k}$ represents the maximum drug import rate related to the species k, and $K_{\mathrm{i},k}$ denotes the concentration of the drug at the half-maximal import rate for this species. Finally, we assume that the saturating drug import function is balanced by a saturating drug export function (as observed in [49, 35]) and that the

rate of export is dependent on the intracellular drug concentration in the following way:

$$E(D_{\text{in},k}) = \frac{V_{\text{e},k} \times D_{\text{in},k}}{K_{\text{e},k} + D_{\text{in},k}}\ , \quad k \in \{\text{S,R}\}\ , \tag{4}$$

where $V_{\text{e},k}$ is the maximum drug export rate related to the species k, and $K_{\text{e},k}$ represents a half-saturation constant for this species.

The dynamics of competition between S and R within a single season begins with the introduction of the drug (D_{ex}) and the limiting nutrient (N) while observing the concentration of both species (X_{S} and X_{R}) in the environment. Note that X_{S} and X_{R} here represent concentrations per ml of unspecified volume but measurable mass. One season of competition of length T is described by the following differential equation:

$$\begin{cases} \dot{N}(t) = -q_{\text{S}}(N(t)) \times X_{\text{S}}(t) - q_{\text{R}}(N(t)) \times X_{\text{R}}(t) \\ \dot{D}_{\text{ex}}(t) = (E(D_{\text{in,S}}(t)) - I(D_{\text{ex}}(t))) \times X_{\text{S}}(t) + (E(D_{\text{in,R}}(t)) - I(D_{\text{ex}}(t))) \times X_{\text{R}}(t) \\ \dot{D}_{\text{in,S}}(t) = (I(D_{\text{ex}}(t)) - E(D_{\text{in,S}}(t))) \times X_{\text{S}}(t) \\ \dot{D}_{\text{in,R}}(t) = (I(D_{\text{ex}}(t)) - E(D_{\text{in,R}}(t))) \times X_{R}(t) \\ \dot{X}_{\text{S}}(t) = G_{\text{S}} \times q_{\text{S}}(N(t)) \times n_{\text{ATP,S}} \times X_{\text{S}}(t) \times i(D_{\text{in,S}}(t)) \\ \dot{X}_{\text{R}}(t) = G_{\text{R}} \times q_{\text{R}}(N(t)) \times n_{\text{ATP,R}} \times X_{\text{R}}(t) \end{cases} \qquad t \in [0,T] \tag{5}$$

The model is parametrised using a system of two human pathogenic species *Candida albicans* and *Candida glabrata* in the presence of an antimicrobial drug fluconazole (see Supplementary Fig 1 and Supplementary Table 1 for details).

We will explore the dynamics of competition over multiple seasons of growth by representing (5) as a discrete dynamical system, Φ, in the following way. At the end of a growth season of length T, a fixed measure of biomass is transferred to a new environment containing replenished growth medium with limiting nutrient concentration N and drug D_{ex}; these are also fixed at the same concentrations at the start of each season. This creates a 1-season map, $\Phi(f;T,m,n)$ where $f = X_{\text{S}}(0)/(X_{\text{S}}(0) + X_{\text{R}}(0))$ is the initial frequency of S at the start of a season and we solve (5) forwards for T units of time with $D_{ex}(0) = m$ and $N(0) = n$. For simplicity, we assume $D_{\text{in,k}}(0) = 0$ for $k \in \{S,R\}$ and we remark on this assumption

below. Given this, $\Phi(f;T,m,n) = X_{\mathrm{S}}(T)/(X_{\mathrm{S}}(T)+X_{\mathrm{R}}(T))$ which is the frequency of S after the season of growth has finished. Repeated applications of Φ to initial frequencies of S can be used to determine *C. albicans* frequency after any number of seasons j, which is typically written $f_j = \Phi(f_{j-1};T,m,n)$ when f_0 is known and (T,m,n) is a vector of parameters that may alter the dynamics induced by Φ if they change. This dynamical systems approach to modelling seasonal microbial populations has been used elsewhere [35, 52].

The assumption that $D_{\mathrm{in,k}}(0) = 0$ is needed so that the discrete dynamical system, Φ, is a well-defined single-season map acting on a 1-dimensional variable f. If this condition on the internal drug concentration were not met, that concentration would also need to be tracked by Φ, making it a 2-dimensional map of a 2-dimensional variable. To avoid this complication, we use this assumption that has the biological interpretation of microbes, that have active drug export systems, being washed free of drug before a new season begins.

As (5) has no concept of cell volume but it can represent biomass, we need a rationale for relating modelled outputs to empirical data where measures may be made on a per cell basis. Therefore, we convert biomass predictions from (5) into cell concentration quantities by making the assumption that empirically determined biomass (optical density (OD), see Supplementary Fig. 1) has a single and fixed conversion parameter that is a proxy for the number of cells per unit of biomass.

The above seasonal dynamic defined by Φ mimics a common experimental protocol known as 'batch culture' but there are other protocols and so, to compare the behaviour of (5) with its equivalent in a chemostat environment, we modified (5) as described in Supplementary Section 4 to have a constant flow of nutrients. Finally, we remark that growth within a single season is dynamic and not necessarily in equilibrium whereas Φ could have itself achieved equilibrium by approaching a fixed point f^*, where $f_* = \Phi(f_*)$.

2.2 Experimental materials and methods

2.2.1 Strains and medium

The *Candida albicans* strain ACT1-GFP was used, which is the SBC153 strain tagged with GFP at the ACT1 locus using a nourseothricin resistance cassette [50]. The wild-type *Candida glabrata* reference strain ATCC2001 was used. Each strain was streaked from glycerol stocks onto YPD agar and incubated for 2 days at 30°C. A stock solution of fluconazole was prepared at 2 mg/ml in DMSO, stored at -20°C and diluted into medium as necessary. Experiments were performed in synthetic complete (SC) media (0.67% w/v yeast nitrogen base without amino acids, 0.079% w/v synthetic complete supplement mixture (Formedium, UK)).

2.2.2 Competitions in varying glucose and fluconazole

Overnight cultures of *C. albicans* or *C. glabrata* were prepared by inoculating a single colony into 5 ml of synthetic complete (SC) medium containing either 0.025%, 0.05%, 0.1%, or 0.5% glucose (weight/volume) and incubating at 30°C and 180 rpm for 16 – 18 hours. Overnight cultures were then mixed to achieve a range of 12 initial fractions of *C. albicans*. Note that this protocol is different from that of Fig. 1b in [35], where overnights were performed in YPD and at a different initial density.

Fluconazole (0, 0.5 μg/ml or 2 μg/ml) was added to SC medium containing either 0.025%, 0.05%, 0.1%, or 0.5% glucose (the same % as in the overnight cultures) and a volume of 145 μl added to the wells of a 96-well flat bottom microtiter plate. Each mixed cell suspension was added (5 μl) to six wells making a total volume of 150 μl in each well (72 wells in total). This resulted in a dilution from the overnights of $\times 30$ allowing a maximum of $\log_2(30) \sim 4.9$ generations of growth until stationary phase. Plates were sealed with adhesive films and two holes were punched above each well with a sterile needle to allow air flow. Plates were incubated at 30°C and 350 rpm for 24 hours. *C. albicans* is a polymorphic fungus, able to grow as yeast, pseudohyphae or hyphae. The growth conditions used were crucial in maintaining it as yeast and therefore allowing a consistent form of quantification across a range of nutrient and drug concentrations.

2.2.3 Flow cytometry measurements

The fraction of each strain in the initial mixtures was determined using flow cytometry. Samples were prepared by adding 5 μl of each mixture to 145 μl of sterile DI water in the wells of a 96-well flat bottom microtiter plate, following the protocol of the test cultures but replacing the medium with water. These suspensions were diluted as necessary in DI water ($2\times$, $3\times$ or $10\times$) to achieve $5 \times 10^4 - 5 \times 10^5$ cell/ml for measurement.

To measure the fraction of *C. albicans* in samples after 6 hours the contents of three of the six replicate mixtures were pipetted vigorously and 30 μl removed for dilution with DI water. The plate was returned to the incubator and the same protocol was repeated with the remaining untouched wells at 24 hours.

A Guava easyCyte HT System using Guava InCyte software (Merck Millipore) was used for flow cytometry to record 5000 events. Using a FSC - SSC plot, events were gated and then strains separated according to their GFP expression (excitation laser (525/30 nm)), to calculate the frequency of *C. albicans* (Supplementary Fig 7). Three wells containing diluted SC medium in water were measured at the end of a run of samples to record the number of false positives in each gate, the averages of which were subtracted from the numbers measured for each test sample. Debris in the medium appears predominately within the gated region for *C. glabrata*. Without this blanking procedure axenic samples of *C. albicans* typically returned 95 – 100% of events in the gated region. Once blanked, this increased to 98 – 100%.

3 Results

We begin by theoretically exploring the behaviour of the system (5). In the absence of drug, our model predictions are consistent with previous competition models [35] parametrised by the same experimental system of two *Candida* species (Supplementary Section 1). In particular, S outcompetes R at low resource concentrations, while the opposite happens at high resource concentrations (see Supplementary Section 2 for details).

Subsequently, we find that for short growth season length (small T), R outcompetes S over a greater range of initial resource concentrations than when season length is long (large T), see Supplementary

Fig 2. As the limiting resource is replenished to its original levels at the beginning of each season, shorter season lengths enable the resource to remain at higher concentrations than when season lengths are longer, thus favouring R. We also find that high population densities favour S for most season lengths, with R having an advantage only at sufficiently high initial resource concentrations (see Supplementary Fig 2 and Supplementary Table 2 for details).

In the presence of drug, introduced into the environment at a fixed concentration at the beginning of each season, the outcome of competition between S and R is illustrated in Fig 1. In particular, for a given drug concentration there are four possible outcomes depending on T and initial concentration of resources: S always outcompetes R (light blue region in Fig 1); R always outcompetes S (gray region in Fig 1); either species can outcompete the other depending on the initial frequency (brown region in Fig 1), and both species can coexist (dark blue region in Fig 1).

The outcome of competition between S and R also changes with the drug concentration in the environment. Fig 2 illustrates a dose-response mosaic (as introduced in [35]) showing the outcome of competition as a function of initial nutrient and drug concentrations as well as how this dose-response mosaic changes for different T. Coexistence between S and R is predicted for both small and large T across a range of drug concentrations, for initial nutrient concentrations at which the S species wins without the drug. This range of nutrient concentrations moves higher as T increases.

Interestingly, we observe three qualitatively different outcomes regarding the relationship between resistance and T. First, for environmental conditions with sufficiently high initial drug concentration and sufficiently low initial resource concentration, increasing T can promote resistance (black squares). Second, the outcome of competition can be independent of T. This is shown in Fig 2 for environmental conditions with intermediate initial drug concentrations and sufficiently high initial resource concentrations (black triangles). In this case the resistant competitor wins, regardless of T. Finally, we observe that decreasing T can promote resistance. This is shown in Fig 2 for environmental conditions with sufficiently low initial drug concentration and intermediate initial resource concentration (black circles). Qualitatively equivalent theoretical results (across slightly different timescales) have been observed in a modelled chemostat environment (cf. Supplementary Fig 6).

Next we seek qualitative confirmation of the trends observed using (5), and Φ, by conducting competition experiments between the sensitive species *C. albicans* (S) and the resistant species *C. glabrata* (R) and monitoring their relative frequencies. For this we co-cultured both species in shaken, 96-well plates containing liquid growth media supplemented with glucose and fluconazole. The plates were inoculated with a mixture of fluorescently labelled *C. albicans*, at proportion f, and *C. glabrata*, at proportion $1-f$. After a fixed growth time T (one season) densities and frequencies of each species were determined using flow cytometry (see Section 2.2). The outcomes of competition were subsequently determined by deploying ideas from microbial population biology [51] and dynamical systems theory, as previously done in [35, 52]. In particular, population dynamics theory states that one can deduce multi-season frequency dynamics from the 'cobweb diagram' determined from the initial *C. albicans* frequency plotted versus the final frequency each season, as we further explain.

The shape of the function $\Phi(f)$ describing a 'single-season frequency change map' for the fixed season length T, the initial drug concentration m and the initial nutrient concentration n (as described in Section 2.1) subsequently determines the outcome of competition [35] with Fig 3 illustrating possible outcomes. Namely, if for each f between 0 and 1, $\Phi(f)$ lies above the diagonal line denoted by $\Phi(f)=f$ (Fig 3, dotted line), then any initial frequency of S will increase over a single season. Thus the fraction of S in the population will increase over multiple seasons until it reaches 1, meaning S wins the competition (Fig 3(a)). If for each f between 0 and 1, $\Phi(f)$ lies below the diagonal line then any initial frequency of S will decrease over a single season. Thus the fraction of S in the population will decrease over multiple seasons until it reaches 0, meaning the resistant species (R) wins the competition (Fig 3 (b)). If there exists an f between 0 and 1 for which $\Phi(f)$ crosses the diagonal, two outcomes are possible: coexistence between S and R (Fig 3 (c)) or bistable exclusion where either species can win depending on their initial frequency (Fig 3 (d)).

Experimentally generated 'cobweb diagrams' for different resource and drug concentrations and season lengths are presented in Fig 4, showing qualitative agreement with the model predictions. In particular, consistent with the model prediction (Fig 2 (a, b), gold and red squares marked A), in the absence of drug, S outcompetes R when T is large, while this is not the case for small T (Fig 4, A). This is observed by noting that the red cobweb diagram is significantly above the diagonal for all initial frequencies (see also

Fig 3 (a) for a theoretical explanation), while this is not the case for the gold cobweb diagram.

Moreover, as predicted by the model (Fig 2 (a, b), gold and red squares marked B), for certain resource and drug concentrations, T has little or no effect on the outcome of competition (Fig 4, B). In that case, R outcompetes S for both long and short season lengths, this can be observed in Fig 4, B, by noting that both gold and red cobweb diagrams are significantly below the diagonal (also see Fig 3 (b) for a theoretical explanation).

Our data also recovers the result predicted by the model that, in the presence of drug, decreasing T favours the resistant species (Fig 4, C, D, E and F). In that case, for large T, R is unable to completely outcompete S, this can be observed in Fig 4, C, D and E by noting that for low initial frequencies red cobweb data is not significantly below the diagonal (negative frequency dependence), indicating possible coexistence between S and R (see Fig 3 (c) for a theoretical explanation), which is also observed in our model Fig 2 (b) (C, D, and E red squares). However, when T is small, R outcompetes S, which is observed in Fig 4, C, D, and E, by noting that for all initial frequencies gold cobweb data is significantly below the diagonal (also see Fig 3 (b) for a theoretical explanation). This mimics the model predictions shown in Fig 2 (a) (C, D, and E gold squares).

4 Discussion

Our study shows that a simple mathematical model of a two-species microbial community where a drug-sensitive and a drug-resistant species compete for a limited nutrient in the presence of a drug, is capable of capturing a rich diversity of competition outcomes, namely, coexistence, competitive exclusion, and bistability. Temporal fluctuations in nutrient and drug concentrations readily experienced in natural environments shape the regions of parameter space for which different competition outcomes are observed over time (Fig 2).

Considering environmental fluctuations is important. Micro-organisms face changes in the concentration of antibiotics during chemotherapeutic treatments, with clinicians varying dosing regimens [11, 12, 13]. Similarly, concentrations of antibiotics change in the environment as antimicrobial compounds are re-

leased by clinical, veterinary, or agricultural practices [53]. Micro-organisms also face changes in nutrient availability at all environmental scales [54]. Glucose concentrations in the blood of critically ill patients can have substantial daily variations [9, 10], while similar rapid fluctuations in dissolved organic carbon are observed in marine environments [55].

Our model achieves good qualitative agreement with empirical observations and its simplicity enables us to probe mechanisms driving the different competition outcomes. The model was parametrised using growth data on clinical isolates of *C. albicans* and *C. glabrata* species. The two species have different metabolism [56] and a previous study showed that, in the absence of drug, this can lead to complex, density- and frequency-dependent ecological interactions such as cheating and cooperation [57]. Here we found that differences in metabolism can enable *C. albicans* to outcompete *C. glabrata* at low resource concentrations, while the opposite can happen at high resource concentrations. Increasing glucose concentration has a higher impact on the relative fitness of S when S is rare than when common, leading to a region of nutrient concentrations characterised by bistability situated between the regions of competitive exclusion. The resource concentration sufficient to support one species over the other depended on the frequency of environmental fluctuations introduced here through changes in the length of the growing season. For short season lengths *C. glabrata* outcompeted *C. albicans* over a greater range of initial resource concentrations than when the length of the growing season was longer (Supplementary Fig 2). Short season lengths lead to a reduced wavelength of fluctuating resource concentration, enabling resources to remain at higher concentrations than when the season length was longer, thus favouring *C. glabrata*, which is better adapted to growth at high resource concentrations.

A drug, fluconazole, was subsequently introduced into the environment with *C. albicans* being susceptible and *C. glabrata* resistant to it. In that case, alongside competitive exclusion and bistability, the model also predicted coexistence as an additional outcome of competition, this has also been observed empirically [35]. Drug is absorbed and affects sensitive species (S) on a timescale relevant to the dynamics of resource consumption and to the season lengths explored here. Whereas the relative fitness of S increases over the growing season due to nutrient depletion, it is also impacted by the drug. In particular, the drug has lower impact on the relative fitness of S when S is rare than when common. When S is initially rare in

the population, R species can act as a sink for the drug in the environment (Supplementary Fig 5). Therefore the average intracellular drug concentration per cell for S is lower in this case than when S is initially common (Supplementary Fig 5). This, coupled with the fact that in the absence of drug S outcompetes R at a low resource concentration, allows S to coexist with R through negative frequency dependence in the presence of drug for sufficiently long growing seasons (see Fig 2 and Supplementary Fig 4).

The mechanism driving coexistence between sensitive and resistant *Candida* species identified here, could be relevant to the coexistence of resistant and sensitive species and strains more broadly. We see coexistence in the presence of drugs at glucose concentrations for which the sensitive species would outcompete the resistant species in the absence of drugs. Frequently mutations that cause a sensitive strain to become resistant are costly to growth in the absence of the drug [58], but may not reduce drug accumulation rate in the presence of the drug (e.g. target modification) [59]. Therefore depending on the nature of the cost of resistance, similar negative frequency dependent interactions to those observed by us here could drive coexistence between sensitive and resistant strains of the same species. This mechanism differs from that seen previously [60, 61, 62, 63] where resistance is linked to a public trait which protects the sensitive strain. In reality, many mechanisms are likely to contribute to the maintenance of both resistance and sensitivity within populations, infections, and hosts, but it is clear from the work we present that nutrients are an important piece of the jigsaw.

Our work also suggests that the speed and therefore mode of drug action could have an impact on the competition outcomes, in particular whether coexistence is observed. The uptake of the antifungal drug fluconazole considered here occurs over a timescale of hours, similar to that of nutrient depletion for our system. However, the uptake and effects of other antifungal drugs may operate over different timescales to those of nutrient depletion, e.g. caspofungin uptake in *C. albicans* saturates within ~ 30 min [64]. Thus an important next step would be to extend our mathematical model and explicitly model drug action and dynamics to examine how different time scales shift or alter the observed outcomes. Nonetheless, this is a challenging proposition, with researchers adopting a range of differing strategies [65, 66, 49, 35].

Given that nutrient depletion and drug uptake are dependent on time, it is perhaps unsurprising that competition outcomes in our system are dependent on frequency of environmental fluctuations. However,

we find the nature of this dependence interesting. By increasing the frequency of environmental fluctuations, often termed disturbance [67], the resistance of the population can decrease, increase or remain unchanged depending on the initial nutrient and drug concentrations in the environment. Most interestingly, for intermediate resource concentrations and sufficiently low drug concentrations a high frequency of disturbance can promote resistance (Fig 2). The empirical environmental conditions for which we validate this result experimentally (Fig 4) mirror glucose concentrations from previous *in vitro Candida* studies [68, 69] and fluconazole concentrations from previous *in vitro* drug-adaptation studies [70].

In our system environmental fluctuations are introduced in a similar manner done elsewhere [71, 72, 73]; after a certain period of growth the majority of the population is discarded and a small fraction is transferred into a new environment containing replenished nutrients and drugs. In this case both the population and ambient conditions (level of nutrient and drug concentrations), experience temporal fluctuations. We also observe qualitatively similar theoretical outcomes in chemostat environments (seen by comparing Fig 2 to Supplementary Fig 6), where the population experiences reduction in size due to mortality events represented by a constant dilution, but changes to nutrient and drug concentrations are not manually introduced.

The observed complex relationship between environmental fluctuations and resistance contrasts with single species studies, where theoretically [74, 75] and empirically [26, 28, 27] it is predicted that decreasing the frequency of environmental fluctuations promotes evolved resistance. While environmental fluctuations can arise from resource fluctuations, increases in drug concentration or drug switching as well as mortality events, our findings have an important consequence. Single species antibiotic resistance assays are a poor predictor of multi-species community dynamics as they do not take into account the impact resources can have on the competition outcomes between sensitive and resistant species. Thus, drug treatments designed to minimise the evolution of resistance in single-species communities, advocating 'in general' fast environmental change, could in a mixed-species context have undesired consequences by promoting resistance.

5 Author Contribution

IG and REB conceived the idea; OAN, REB and IG developed the model; OAN analysed and parametrised the model and performed numerical simulations; AJ designed and conducted the experiments; OAN, AJ, REB, and IG wrote the manuscript

6 Acknowledgements

We would like to thank Richard Lindsay, Emily Cook and Alan Brown for helpful discussions.

7 Data Accessibility

The research data supporting this publication can be found at https://doi.org/10.24378/exe.2323

8 Funding Statement

OAN, AJ, and IG were funded by an ERC Consolidator grant (MathModExp 647292) to IG, REB was funded by an EPSRC Healthcare Technology Impact Fellowship (EP/N033671/1).

Figure Legends

Figure 1: The outcome of competition between S and R predicted by the model (5). Competition outcomes in the presence of drug as a function of the initial nutrient concentration N and the season length T (we set $D(0) = 1$ μg/ml as an illustration, however the results do not qualitatively change for $D(0) = 0.5$ or $D(0) = 2$ μg/ml). Inside the light-blue region S wins, R wins inside the light-gray region, while 'bistable exclusion' occurs in the brown region, and both species coexist in the dark-blue region. Initial population densities are (a) 10^4, (b) 10^6, and (c) 10^7 cells/ml. Each axis corresponding to the initial nutrient concentration is plotted from 0.95% to 1.7% glucose.

Figure 2: Theoretical dose-response mosaics describing the outcomes of competition between sensitive and resistant species. Theoretical two-dimensional dose-response mosaics describing the outcomes of competition between sensitive and resistant species at varying initial nutrient and drug concentrations within one growing season of two different lengths: (a) short, corresponding to the high frequency of nutrient and drug fluctuations, (b) and long, corresponding to the low frequency of nutrient and drug fluctuations. Results are obtained by means of the model's (5) simulations with the parameters values taken from Supplementary Table 1 and the initial community density fixed at 10^6 cells/ml value. Each axis corresponding to the initial nutrient concentration runs from 1.3% to 1.5% glucose, and each axis corresponding to the initial drug concentration is plotted from 0 μg/ml to 12 μg/ml fluconazole. Letters A - F are for comparison with the experimental results presented in Figure 4.

Figure 3: Theoretically generated 'cobweb diagrams'. Population dynamics theory states that one can deduce multi-season competition dynamics between *C. albicans* (S) and *C. glabrata* (R) from the 'cobweb diagrams' determined from the initial frequency of S species plotted versus its final frequency each season. (a) If $\Phi(f)$ lies above the diagonal for all f between 0 and 1, then S wins; (b) if $\Phi(f)$ lies below the diagonal for all f between 0 and 1, then R wins; (c) if there exists a special frequency, $f_\star$, which lies on the diagonal line, and $\Phi(f) > f$ for $0 < f < f_\star$ while $\Phi(f) < f$ for $f_\star < f < 1$, then the two species coexist (for example, both starting frequencies of A and B will converge to frequency $f_\star$); (d) if there exists a special frequency, $f_{\star\star}$, which lies on the diagonal line, and $\Phi(f) < f$ for $0 < f < f_{\star\star}$ while $\Phi(f) > f$ for $f_{\star\star} < f < 1$, then either species can dominate depending on their initial frequencies: if the initial fre-

quency of S is smaller than $f_{\star\star}$ (for example, for starting frequency C) then S loses out in competition to R, otherwise R loses out (for example, for starting frequency D) - this is 'bistable exclusion'.

Figure 4: Experimentally generated 'cobweb diagrams'. Experimental two-dimensional dose-response mosaic for the conditions (A, D, B) 0.05% glucose + (0, 0.5, 2) μg/ml fluconazole and (C, E, F) (0.025, 0.1, 0.5) % glucose + 0.5 μg/ml fluconazole. For each condition (shown in panels A – F) the outcome of competition is measured for season lengths corresponding to the long and short seasons used in the mathematical simulations. Empirically, the short season is 6 hours in length (data shown in gold) and the long season is 24 hours in length (data shown in red) corresponding to ~ 3 generations and ~ 5 generations of single species growth respectively. A 'single-season frequency change map' with the initial frequency of *C. albicans* is plotted on the x-axis and the final frequency of *C. albicans* – on the y-axis. Gray lines link the average (large marker) of 3 replicate samples (small marker) and error bars are the 95% CI (confidence interval). The diagonal dashed line represents no change in fraction. **Gold data (B, E)** is significantly below the diagonal (significance judged at $p < 0.05$, two-sample, two-sided, t-test with unequal variance between three replicate measurements of the initial fraction and three biological replicates of the final fraction) at every initial fraction ($t > 4.784$, $p < 0.0339$, where $\delta f =$ average initial fraction of S - average final fraction of S < 0), **(A, C, D, F)** is significantly below the diagonal ($t > 4.014$, $p < 0.0444$) or shows no significant deviation from the diagonal ($^{+}t < 3.077$, $p > 0.0547$). **Red data (A)** all fractions are significantly above the diagonal ($t > 3.647$, $p < 0.0437$, where $\delta f > 0$) except at an initial fraction of 0.78 ($^{++}t = 3.473$, $p = 0.0673$), **(B)** is below the diagonal at every initial fraction ($t > 7.091$, $p < 0.0184$), **(C)** initial fractions ≤ 0.29 are significantly above the diagonal ($t > 4.390$, $p < 0.0120$), while initial fractions ≥ 0.42 do not deviate from the diagonal with any significance ($t < 1.876$, $p > 0.242$), **(D)** initial fractions in the range 0.73 – 0.93 are below the diagonal ($t > 4.361$, $p < 0.0248$) while initial fractions ≤ 0.64 do not significantly deviate from the diagonal ($t < 3.020$, $p > 0.0535$), **(E)** initial fractions ≥ 0.67 are significantly below the diagonal ($t > 4.207$, $p < 0.0381$), while fractions ≤ 0.47 do not deviate significantly from the diagonal ($t < 2.309$, $p > 0.0856$), **(F)** initial fractions ≥ 0.45 are significantly below the diagonal ($t > 4.622$, $p < 0.0178$), while initial fractions ≤ 0.37 do not deviate significantly from the diagonal ($t < 3.440$, $p > 0.0533$).

Figures

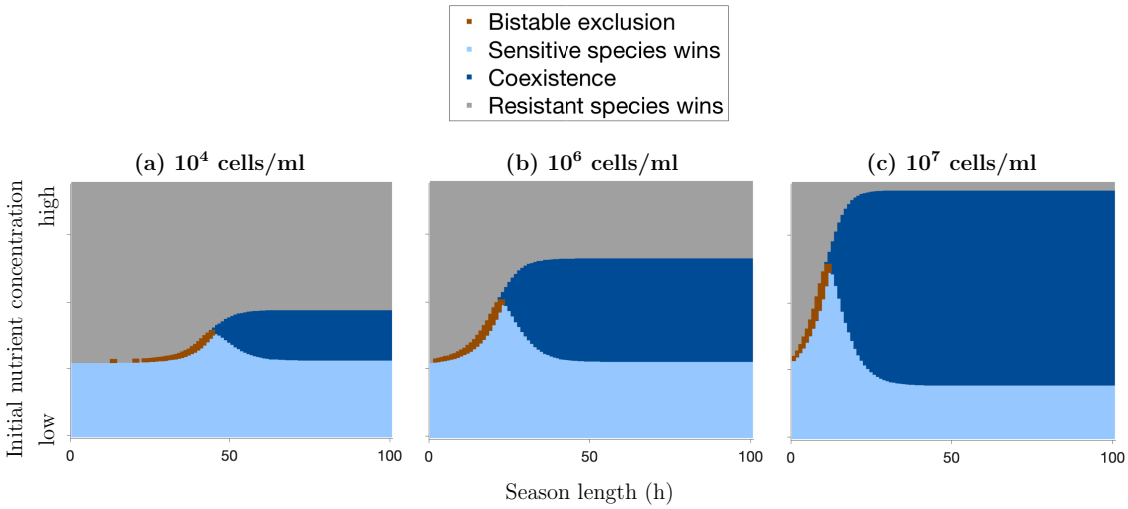

Figure 1

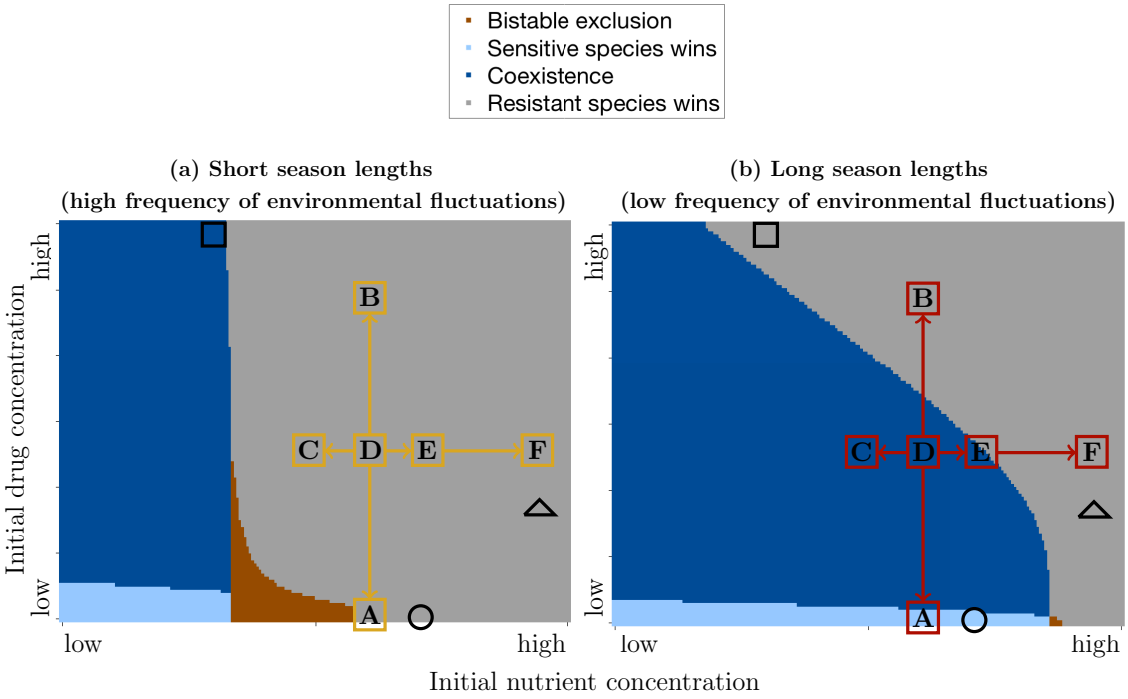

Figure 2

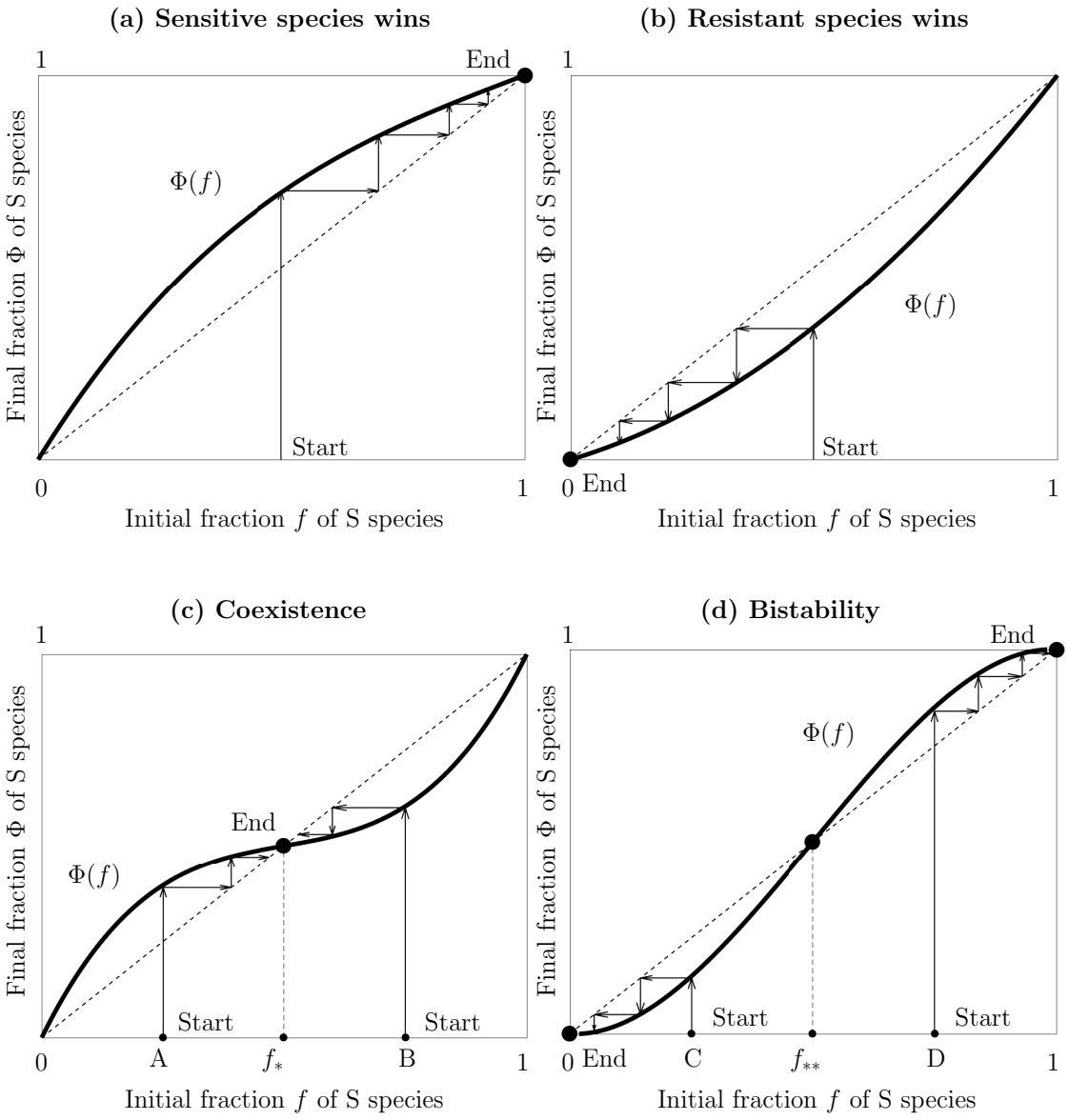
(a) Sensitive species wins
(b) Resistant species wins
(c) Coexistence
(d) Bistability
Final fraction Φ of S species
Initial fraction f of S species
$\Phi(f)$
Start
End
0
1
A
f_*
B
C
f_{**}
D

Figure 3

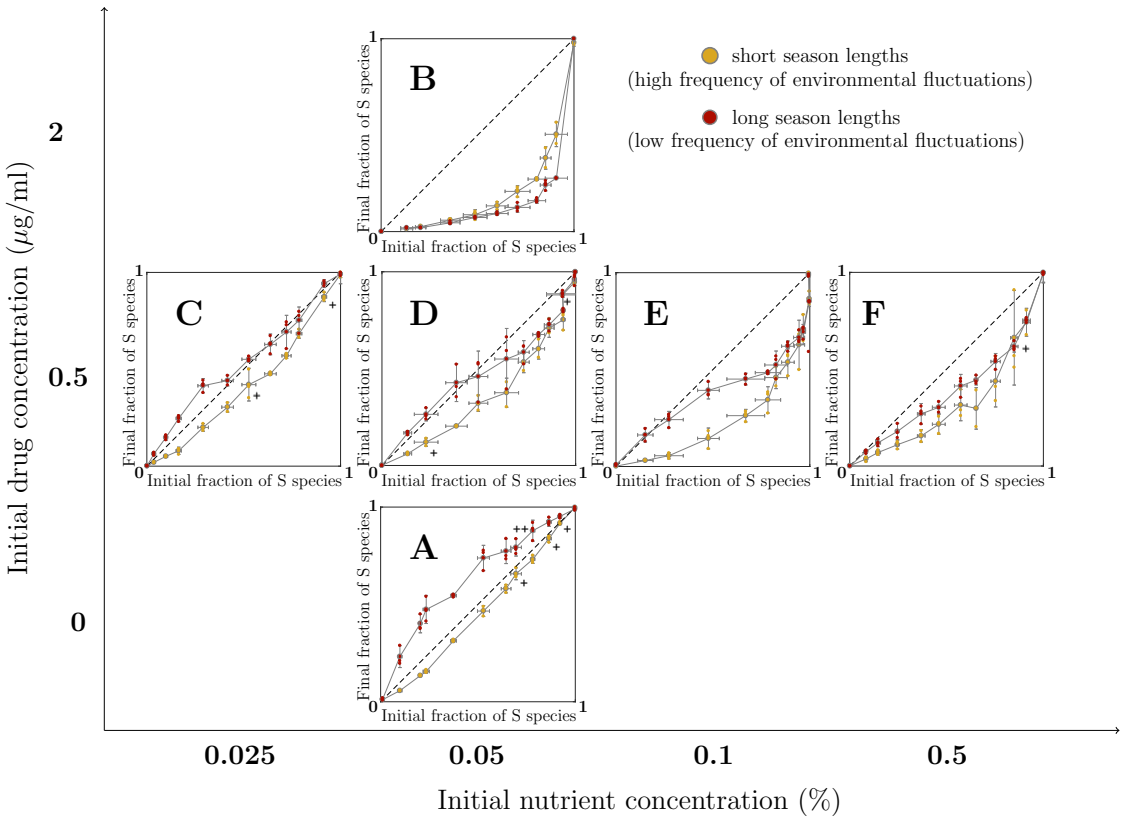
short season lengths
(high frequency of environmental fluctuations)
long season lengths
(low frequency of environmental fluctuations)
A
B
C
D
E
F
Final fraction of S species
Initial fraction of S species
0
1
2
0.5
Initial drug concentration (μg/ml)
0.025
0.05
0.1
0.5
Initial nutrient concentration (%)

Figure 4

References

[1] Structure, function and diversity of the healthy human microbiome. Nature. 2012;486(7402):207–214.

[2] Stinson LF, Boyce MC, Payne MS, Keelan JA. The Not-so-Sterile Womb: Evidence That the Human Fetus Is Exposed to Bacteria Prior to Birth. Frontiers in microbiology. 2019;10:1124.

[3] Turnbaugh PJ, Ridaura VK, Faith JJ, Rey FE, Knight R, Gordon JI. The Effect of Diet on the Human Gut Microbiome: A Metagenomic Analysis in Humanized Gnotobiotic Mice. Science Translational Medicine. 2009;1(6):6ra14.

[4] Wu GD, Chen J, Hoffmann C, Bittinger K, Chen YY, Keilbaugh SA, et al. Linking Long-Term Dietary Patterns with Gut Microbial Enterotypes. Science. 2011;334(6052):105–108.

[5] David LA, Maurice CF, Carmody RN, Gootenberg DB, Button JE, Wolfe BE, et al. Diet rapidly and reproducibly alters the human gut microbiome. Nature. 2014;505(7484):559–563.

[6] Jakobsson HE, Jernberg C, Andersson AF, Sjölund-Karlsson M, Jansson JK, Engstrand L. Short-term antibiotic treatment has differing long-term impacts on the human throat and gut microbiome. PLoS One. 2010;5(3):e9836.

[7] Cowart SL, Stachura ME. Glucosuria. Butterworth Publishers, a division of Reed Publishing; 1990.

[8] Ferraris RP, Yasharpour S, Lloyd KC, Mirzayan R, Diamond JM. Luminal glucose concentrations in the gut under normal conditions. American Journal of Physiology-Gastrointestinal and Liver Physiology. 1990;259(5):G822–G837.

[9] Carlotti AP, Bohn D, Jankiewicz N, Kamel KS, Davids MR, Halperin ML. A hyperglycaemic hyperosmolar state in a young child: diagnostic insights from a quantitative analysis. QJM. 2007;100(2):125–137.

[10] Manoj M, George MR, Dipu R, Jishnu J. The survival story of a diabetic ketoacidosis patient with blood sugar levels of 1985 mg/dl. Asian J Med Sci. 2017;8:60–61.

[11] McFarland LV, Elmer GW, Surawicz CM. Breaking the Cycle: Treatment Strategies for 163 Cases of Recurrent *Clostridium difficile* Disease. Am J Gastroenterol. 2002;97(7):1769–1775.

[12] Cousin L, Berre ML, Launay-Vacher V, Izzedine H, Deray G. Dosing guidelines for fluconazole in patients with renal failure. Nephrol Dial Transplant. 2003;18:2227–2231.

[13] Ashbee HR, Barnes RA, Johnson EM, Richardson MD, Gorton R, Hope WW. Therapeutic drug monitoring (TDM) of antifungal agents: guidelines from the British Society for Medical Mycology. J Antimicrob Chemother. 2014;69:1162–1176.

[14] Matzke GR, Zhanel GG, Guay DRP. Clinical Pharmacokinetics of Vancomycin. Clinical Pharmacokinetics. 1986;11(4):257–282.

[15] Levy SB. Antibiotic resistance: an ecological imbalance. Ciba Found Symp. 1997;207:1–9.

[16] Lehtinen S, Blanquart F, Croucher NJ, Turner P, Lipsitch M, Fraser C. Evolution of antibiotic resistance is linked to any genetic mechanism affecting bacterial duration of carriage. PNAS. 2017;114(5):1075–1080.

[17] Davies NG, Flasche S, Jit M, Atkins KE. Within-host dynamics shape antibiotic resistance in commensal bacteria. Nat Ecol Evol. 2019;3:440–449.

[18] Boktour MR, Kontoyiannis DP, Hanna HA, Hachem RY, Girgawy E, Bodey GP, et al. Multiple-species candidemia in patients with cancer. Cancer. 2004;101(8):1860–1865.

[19] Samaranayake LP, MacFarlane TW, Williamson MI. Comparison of Sabouraud dextrose and Pagano-Levin agar media for detection and isolation of yeasts from oral samples. J Clin Microbiol. 1987;25(1):162–164.

[20] Weaver VB, Kolter R. *Burkholderia* spp. Alter *Pseudomonas aeruginosa* Physiology through Iron Sequestration. Journal of Bacteriology. 2004;186(8):2376–2384.

[21] Kussell E, Leibler S. Phenotypic Diversity, Population Growth, and Information in Fluctuating Environments. Science. 2005;309(5743):2075–2078.

[22] Cvijović I, Good BH, Jerison ER, Desai MM. Fate of a mutation in a fluctuating environment. Proceedings of the National Academy of Sciences. 2015;112(36):E5021–E5028.

[23] Sæther BE, Engen S. The concept of fitness in fluctuating environments. Trends in Ecology & Evolution. 2015;30(5):273–281.

[24] Svardal H, Rueffler C, Hermisson J. A general condition for adaptive genetic polymorphism in temporally and spatially heterogeneous environments. Theoretical Population Biology. 2015;99:76–97.

[25] Salignon J, Richard M, Fulcrand E, Duplus-Bottin H, Yvert G. Genomics of cellular proliferation in periodic environmental fluctuations. Molecular Systems Biology. 2018;14(3):e7823.

[26] Perron GG, Gonzalez A, Buckling A. The rate of environmental change drives adaptation to an antibiotic sink. J Evol Biol. 2008;21:1724–1731.

[27] Roemhild R, Gokhale CS, Dirksen P, Blake C, Rosenstiel P, Traulsen A, et al. Cellular hysteresis as a principle to maximize the efficacy of antibiotic therapy. PNAS. 2018;115(39):9767–9772.

[28] Lindsey HA, Gallie J, Taylor S, Kerr B. Evolutionary rescue from extinction is contingent on a lower rate of environmental change. Nature. 2013;494:463–467.

[29] Stomp M, van Dijk MA, van Overzee HMJ, Wortel MT, Sigon CAM, Egas M, et al. The Timescale of Phenotypic Plasticity and Its Impact on Competition in Fluctuating Environments. The American Naturalist. 2008;172(5):E169–E185.

[30] Chesson PL. Coexistence of competitors in spatially and temporally varying environments: A look at the combined effects of different sorts of variability. Theoretical Population Biology. 1985;28(3):263–287.

[31] Comins HN, Noble IR. Dispersal, Variability, and Transient Niches: Species Coexistence in a Uniformly Variable Environment. The American Naturalist. 1985;126(5):706–723.

[32] Kremer CT, Klausmeier CA. Species packing in eco-evolutionary models of seasonally fluctuating environments. Ecology Letters. 2017;20(9):1158–1168.

[33] Sakavara A, Tsirtsis G, Roelke DL, Mancy R, Spatharis S. Lumpy species coexistence arises robustly in fluctuating resource environments. Proceedings of the National Academy of Sciences of the United States of America. 2018;115(4):738–743.

[34] Gabaldón C, Montero-Pau J, Carmona MJ, Serra M. Life-history variation, environmental fluctuations and competition in ecologically similar species: modeling the case of rotifers. Journal of Plankton Research. 2015;37(5):953–965.

[35] Beardmore RE, Cook E, Nilsson S, Smith AR, Tillmann A, Esquivel BD, et al. Drug-mediated metabolic tipping between antibiotic resistant states in a mixed-species community. Nat Ecol Evol. 2018;2:1312–1320.

[36] Ho-Km, Cheng-Ts. Common Superficial Fungal Infections – a Short Review. Med Bull. 2010;15(11):23–27.

[37] Wenzel RP, Gennings C. Bloodstream infections due to *Candida* species in the intensive care unit: identifying especially high-risk patients to determine prevention strategies. Clin Infect Dis. 2005;41(Suppl. 6):S389–S393.

[38] Brown GD, Denning DW, Gow NA, Levitz SM, Netea MG, White TC. Hidden Killers: Human Fungal Infections. Sci Transl Med. 2012;4(165):165rv113.

[39] Kett DH, Azoulay E, Echeverria PM, Vincent JL. *Candida* bloodstream infections in intensive care units: analysis of the extended prevalence of infection in intensive care unit study. Crit Care Med. 2011;39(4):665–670.

[40] Pappas PG, Rex JH, Sobel JD, Filler SG, Dismukes WE, Walsh TJ, et al. Guidelines for Treatment of Candidiasis. Clin Infect Dis. 2004;38:161–189.

[41] Yang Y-L, Chu W-L, Lin C-C, Tsai S-H, Chang T-P, Lo H-J. An emerging issue of mixed yeast cultures. J Microbiol Immunol Infect. 2014;47:339–344.

[42] Silva S, Henriques M, Hayes A, Oliveira R, Azeredo J, Williams DW. *Candida glabrata* and *Candida albicans* co-infection of an in vitro oral epithelium. J Oral Pathol Med. 2011;40(5):421–427.

[43] Alves CT, Wei XQ, Silva S, Azeredo J, Henriques M, Williams DW. *Candida albicans* promotes invasion and colonisation of *Candida glabrata* in a reconstituted human vaginal epithelium. J Infect. 2014;69(4):396–407.

[44] Rex JH, Pfaller MA, Galgiani JN, Bartlett MS, Espinel-Ingroff A, Ghannoum MA, et al. Development of Interpretive Breakpoints for Antifungal Susceptibility Testing: Conceptual Framework and Analysis of In Vitro–In Vivo Correlation Data for Fluconazole, Itraconazole, and Candida Infections. Clin Infect Dis. 1997;24:235–247.

[45] Pfeiffer T, Schuster S, Bonhoeffer S. Cooperation and Competition in the Evolution of ATP-Producing Pathways. Science. 2001;292:504–507.

[46] Gudelj I, Beardmore RE, Arkin SS, MacLean RC. Constraints on microbial metabolism drive evolutionary diversification in homogeneous environments. J Evol Biol. 2007;20:1882–1889.

[47] Bauchop T, Elsden SR. The Growth of Micro-organisms in Relation to their Energy Supply. J Gen Microbiol. 1960;23:457–469.

[48] Pfeiffer T, Bonhoeffer S. Evolution of Cross-Feeding in Microbial Populations. Am Nat. 2004;163(6):E126–E135.

[49] Mansfield BE, Oltean HN, Oliver BG, Hoot SJ, Leyde SE, Hedstrom L, et al. Azole Drugs Are Imported By Facilitated Diffusion in *Candida albicans* and Other Pathogenic Fungi. PLoS Pathog. 2010;6(9):e1001126.

[50] Milne SW, Cheetham J, Lloyd D, Aves S, Bates S. Cassettes for PCR-mediated gene tagging in *Candida albicans* utilizing nourseothricin resistance. Yeast. 2011;28(12):833–841.

[51] Hibbing ME, Fuqua C, Parsek MR, Peterson SB. Bacterial competition: surviving and thriving in the microbial jungle. Nat Rev Microbiol. 2010;8(1):15–25.

[52] Ribeck N, Lenski RE. Modeling and quantifying frequency-dependent fitness in microbial populations with cross-feeding interactions. Evolution. 2014;69(5):1303–1320.

[53] Levy SB. Factors impacting on the problem of antibiotic resistance. J Antimicrob Chemother. 2002;49:25–30.

[54] Odum WE, Odum EP, Odum HT. Nature's pulsing paradigm. Estuaries. 1995;18:547.

[55] Regier P, Jaffé R. Short-Term Dissolved Organic Carbon Dynamics Reflect Tidal, Water Management, and Precipitation Patterns in a Subtropical Estuary. Front Mar Sci. 2016;3:250.

[56] Ene IV, Brunke S, Brown AJP, Hube B. Metabolism in Fungal Pathogenesis. Cold Spring Harb Perspect Med. 2014;4(12):a019695.

[57] MacLean RC, Gudelj I. Resource competition and social conflict in experimental populations of yeast. Nature. 2006;441:498–501.

[58] Melnyk AH, Wong A, Kassen R. The fitness costs of antibiotic resistance mutations. Evol Appl. 2015;8(3):273–283.

[59] Blair JMA, Webber MA, Baylay AJ, Ogbolu DO, Piddock LJV. Molecular mechanisms of antibiotic resistance. Nature Reviews Microbiology. 2015 jan;13(1):42–51.

[60] Yurtsev EA, Chao HX, Datta MS, Artemova T, Gore J. Bacterial cheating drives the population dynamics of cooperative antibiotic resistance plasmids. Mol Syst Biol. 2013;9.

[61] Lee HH, Molla MN, Cantor CR, Collins JJ. Bacterial charity work leads to population-wide resistance. Nature. 2010;467(7311):82–85.

[62] Dugatkin LA, Perlin M, Lucas JS, Atlas R. Group-beneficial traits, frequency-dependent selection and genotypic diversity: an antibiotic resistance paradigm. Proc Biol Sci. 2005;272(1558):79–83.

[63] Frost I, Smith WPJ, Mitri S, Millan AS, Davit Y, Osborne JM, et al. Cooperation, competition and antibiotic resistance in bacterial colonies. The ISME Journal. 2018;12(6):1582–1593.

[64] Paderu P, Park S, Perlin DS. Caspofungin uptake is mediated by a high-affinity transporter in *Candida albicans*. Antimicrob Agents Chemother. 2004;48(10):3845–3849.

[65] Hanly TJ, Henson MA. Dynamic metabolic modeling of a microaerobic yeast co-culture: predicting and optimizing ethanol production from glucose/xylose mixtures. Biotechnol Biofuels. 2013;6(1):44.

[66] Nicoloff H, Hjort K, Levin BR, Andersson DI. The high prevalence of antibiotic heteroresistance in pathogenic bacteria is mainly caused by gene amplification. Nat Microbiol. 2019;4(3):504–514.

[67] Sousa WP. The Role of Disturbance in Natural Communities. Annu Rev Ecol Syst. 1984;15:353–391.

[68] Baillie GS, Douglas LJ. Iron-Limited Biofilms of *Candida albicans* and Their Susceptibility to Amphotericin B. Antimicrob Agents Chemother. 1998;42(8):2146–2149.

[69] Basson NJ. Competition for glucose between *Candida albicans* and oral bacteria grown in mixed culture in a chemostat. J Med Microbiol. 2000;49(11):969–975.

[70] Huang M, McClellan M, Berman J, Kao KC. Evolutionary Dynamics of *Candida albicans* during *In Vitro* Evolution. Eukaryot Cell. 2011;10(11):1413–1421.

[71] Brockhurst MA, Buckling A, Gardner A. Cooperation Peaks at Intermediate Disturbance. Curr Biol. 2007;17:761–765.

[72] Travisano M, Velicer GJ. Strategies of microbial cheater control. Trends Microbiol. 2004;12(2):72–78.

[73] Zhou L, Slamti L, Nielsen-LeRoux C, Lereclus D, Raymond B. The social biology of quorum sensing in a naturalistic host pathogen system. Curr Biol. 2014;24(20):2417–2422.

[74] Pease CM, Lande R, Bull JJ. A Model of Population Growth, Dispersal and Evolution in a Changing Environment. Ecology. 1989;70(6):1657–1664.

[75] Collins S, de Meaux J, Acquisti C. Adaptive Walks Toward a Moving Optimum. Genetics. 2007;176:1089–1099.

Supplementary Information for:

Predicting community dynamics of antibiotic sensitive and resistant species in fluctuating environments

Olga A. Nev, Alys Jepson, Robert E. Beardmore, and Ivana Gudelj

1 Parameter estimation

Yeasts can use two different pathways to produce ATP from glucose, namely respiration and fermentation [1]. *C. albicans* is a Crabtree-negative species [2] which deploys respiration as a glucose-utilisation strategy, whereby most of its glucose is utilised through the tricarboxylic acid (TCA) cycle to generate biomass and CO_2 [8]. Consistent with published estimates for Crabtree-negative species [3] we fix ATP yield per unit of glucose $n_{\mathrm{ATP,S}} = 28$ pmol ATP/pmol glucose.

In contrast, *C. glabrata* is a Crabtree-positive species [2] which ferments most of the glucose to generate ethanol as bi-product [8]. They produce 2 ATP per glucose in respiration and ~ 18 ATP per glucose in fermentation [1]. At sufficiently low levels of oxygen and glucose, yeasts balance between fermentation and respiration [1]. Therefore we fix ATP yield per unit of glucose $n_{\mathrm{ATP,R}} = 10$ pmol ATP/pmol glucose, as an average of ATP produced during respiration and fermentation.

The growth kinetics parameters, associated with *C. albicans* (*C. glabrata*), namely $V_{\mathrm{max,S}}$, $K_{\mathrm{m,S}}$, and G_{S} ($V_{\mathrm{max,R}}$, $K_{\mathrm{m,R}}$, and G_{R}) were estimated by fitting numerical solutions of the system (5) from the main text describing microbial population growth with $X_{\mathrm{R}} = D_{\mathrm{ex}} = D_{\mathrm{in,S}} = D_{\mathrm{in,R}} = 0$ ($X_{\mathrm{S}} = D_{\mathrm{ex}} = D_{\mathrm{in,S}} = D_{\mathrm{in,R}} = 0$) to empirically obtained *C. albicans* (*C. glabrata*) data (Supplementary Fig 1) previously reported in [9]. Initial parameter guesses for the fitting procedures were guided by parameter estimates from the previous study [9] deploying a similar, although more complex competition model between *C. albicans* and *C. glabrata*.

The drug import/export and inhibition parameters for both *C. albicans* and *C. glabrata* were taken from the literature [9].

All parameter values associated with the model (5) from the main text are summarised in Supplementary Table 1. Our parameterised model is subsequently able to capture previously published experimental results presented in Fig 1 (b) in [9], demonstrating that in the absence of drug, *C. albicans* wins the competition at low glucose concentrations while *C. glabrata* wins the competition at high glucose concentrations (see Fig 2 in the main text).

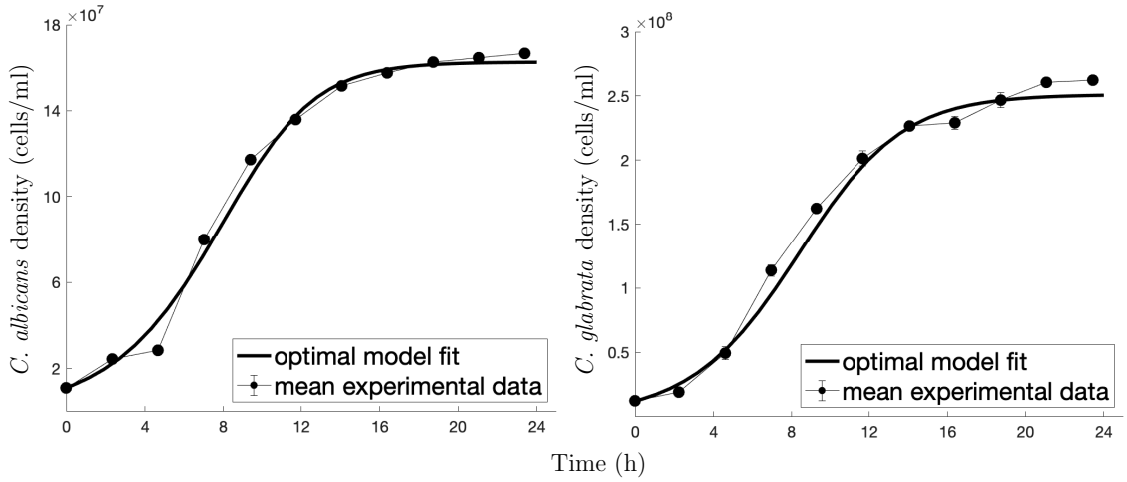

Supplementary Figure 1: Individual growth of *C. albicans* and *C. glabrata* over 24 h in 96-well plates containing the synthetic complete (SC) medium with 2% glucose and no fluconazole. As described in [9] the plate was incubated at 30°C with shaking over 24h and growth monitored by measuring the absorbance of the cell suspensions at 650nm (A650). Absorbance units were converted into number of cells per ml using a single fixed conversion parameter, w, with $w = 1.2 \times 10^8$ for *C. albicans* and $w = 2.2 \times 10^8$ for *C. glabrata*. Left: experimental *C. albicans* growth data (dots, error bars are mean $\pm$ standard error, $n = 3$) together with the optimal non-linear least-squares fit of the system (5) from the main text (solid curve) with $X_R = D_{ex} = D_{in,S} = D_{in,R} = 0$. Estimated growth parameters are: $V_{max,S} = 0.0124395$ pmol/cell/min, $K_{m,S} = 2.60284 \times 10^8$ pmol/ml, $G_S = 0.0488024$ cell/pmol ATP (for datafit statistics please see Supplementary Table 2). Right: experimental *C. glabrata* growth data (dots, error bars are mean $\pm$ standard error, $n = 2$) together with the optimal non-linear least-squares fit of the system (5) from the main text (solid curve) with $X_S = D_{ex} = D_{in,S} = D_{in,R} = 0$. Estimated growth parameters are: $V_{max,R} = 0.0258526$ pmol/cell/min, $K_{m,R} = 10^9$ pmol/ml, $G_R = 0.215259$ cell/pmol ATP (for datafit statistics please see Supplementary Table 2). Optimal parameters values for both species are obtained using *Mathematica's* build in toolbox *NonlinearModelFit*.

Supplementary Table 1: Parameters values of the model (5) from the main text used in this study.

Parameter	Biological interpretation	Value	Units
Growth parameters			
$V_{\mathrm{max,S}}$	maximum glucose uptake rate related to *C. albicans*	0.0124395	pmol/cell/min
$K_{\mathrm{m,S}}$	glucose half-saturation constant related to *C. albicans*	2.60284×10^{8}	pmol/ml
$n_{\mathrm{ATP,S}}$	ATP yield per unit of glucose by *C. albicans*	28	pmol ATP/pmol glucose
G_{S}	biomass yield per unit of ATP by *C. albicans*	0.0488024	cell/pmol ATP
$V_{\mathrm{max,R}}$	maximum glucose uptake rate related to *C. glabrata*	0.0258526	pmol/cell/min
$K_{\mathrm{m,R}}$	glucose half-saturation constant related to *C. glabrata*	10^{9}	pmol/ml
$n_{\mathrm{ATP,R}}$	ATP yield per unit of glucose by *C. glabrata*	10	pmol ATP/pmol glucose
G_{R}	biomass yield per unit of ATP by *C. glabrata*	0.215259	cell/pmol ATP
Drug import parameters			
$V_{\mathrm{i,S}}$	maximum fluconazole import rate related to *C. albicans*	6.55×10^{-9}	pmol/cell/min
$K_{\mathrm{i,S}}$	fluconazole half-saturation constant related to *C. albicans*	6×10^{4}	pmol/ml
$V_{\mathrm{i,R}}$	maximum fluconazole import rate related to *C. glabrata*	9.8×10^{-9}	pmol/cell/min
$K_{\mathrm{i,R}}$	fluconazole half-saturation constant related to *C. glabrata*	1.6×10^{4}	pmol/ml
Drug export parameters			
$V_{\mathrm{e,S}}$	maximum fluconazole export rate related to *C. albicans*	2×10^{-11}	pmol/cell/min
$K_{\mathrm{e,S}}$	fluconazole half-saturation constant related to *C. albicans*	5.8	pmol/ml
$V_{\mathrm{e,R}}$	maximum fluconazole export rate related to *C. glabrata*	3.9×10^{-11}	pmol/cell/min
$K_{\mathrm{e,R}}$	fluconazole half-saturation constant related to *C. glabrata*	0.7	pmol/ml
Drug inhibition parameters			
a	relates to *C. albicans* fluconazole resistance properties	0.52059	dimensionless
b	relates to *C. albicans* fluconazole resistance properties	12.001	pmol/ml
c	relates to *C. albicans* fluconazole resistance properties	5.2347	dimensionless

2 Competition in the absence of drug

In the absence of drug, the outcome of competition between the sensitive (S) and resistant (R) competitors depends on the initial nutrient concentration and the initial population density at the beginning of each season as well as on the season length T (Supplementary Fig 2). Consistent with previous S-R competition models parametrised by these species [9], S outcompetes R at low nutrient concentrations, while the opposite happens at high nutrient concentrations. Note that we are not aware of a mechanism specif-

Supplementary Table 2: Statistics for the estimated growth parameters values

Parameter	Estimate	Standard Error	t-Statistics	P-Value
Growth parameters for *C. albicans*				
$V_{\max,S}$	0.0124395	0.0010896	11.4166	9.08443×10^{-29}
$K_{m,S}$	2.60284×10^{8}	3.0538×10^{7}	8.5233	4.46797×10^{-17}
G_S	0.0488024	0.000115881	421.141	0
Growth parameters for *C. glabrata*				
$V_{\max,R}$	0.0258526	0.0088575	2.91872	0.00361071
$K_{m,R}$	10^{9}	3.74241×10^{8}	2.67208	0.00768775
G_R	0.215259	0.000649799	331.27	0

ically linking resistance and better performance at high nutrient concentrations. However, these species have different modes of metabolism of the single limiting resource they compete for, namely glucose (see Supplementary Section 1 for details). In general, Crabtree-positive yeasts use fermentation even in the presence of oxygen, a strategy thought to have evolved in high sugar environments around the time that fruiting plants emerged [4, 1]. This suggests that R may have spent some of its evolutionary history in high glucose environment, thus having higher growth rates than species S in high glucose environments (see Supplementary Fig 3). This is also consistent with recent observations that our R species (*C. glabrata*) is more frequently isolated from infections of diabetic patients with high blood sugar levels [5, 6]. Species S has a higher growth rate than R when glucose is scarce (Supplementary Fig 3) in line with respiration being more efficient than fermentation (Supplementary Section 1).

For a given T, we also find that increasing initial population density increases the maximal nutrient concentrations ($N_{S,max}$, black dashed line in Supplementary Fig 2) for which S outcompetes R, and increases the minimal nutrient concentration ($N_{R,min}$, white dashed line in Supplementary Fig 2) for which R outcompetes S.

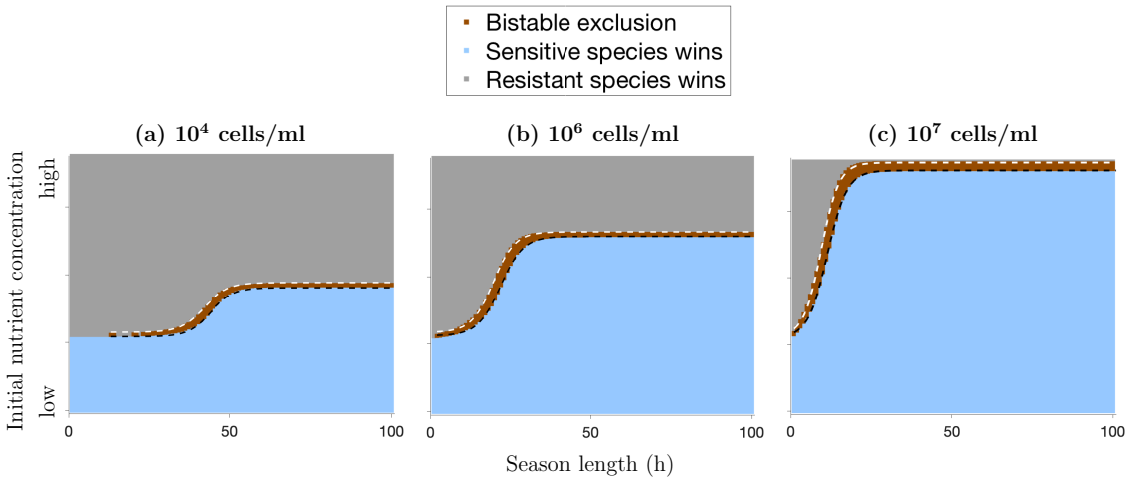

Supplementary Figure 2: The outcome of competition between S and R predicted by the model (5) from the main text. Competition outcomes in the absence of drug (namely, when $D(0) = D_{ex} = D_{in,S} = D_{in,R} = 0$) as a function of the initial nutrient concentration N and the season length T. Inside the light-blue region S wins, R wins inside the light-gray region, while 'bistable exclusion' occurs in the brown region. The black dashed line denotes the maximal nutrient concentrations ($N_{S,max}$) for which S outcompetes R, while the white dashed line denotes the minimal nutrient concentration ($N_{R,min}$) for which R outcompetes S. Initial population densities are (a) 10^4, (b) 10^6, and (c) 10^7 cells/ml. The initial nutrient concentration axis is plotted from 0.95% to 1.7% glucose.

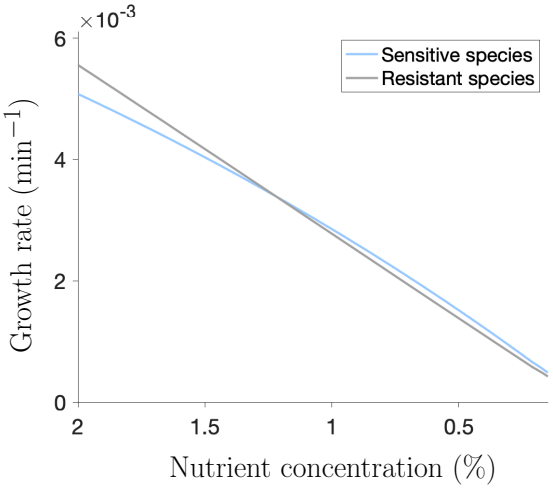

Supplementary Figure 3: Specific growth rates of *C. albicans* and *C. glabrata* in a competition initiated at fractions 0.5:0.5 over 24 h in an initial glucose concentration of 2% without fluconazole. Results are obtained by simulating the model (5) from the main text with parameter values from Supplementary Table 1 and an initial density of 10^6 cell/ml.

In addition, both $N_{\mathrm{S,max}}$ and $N_{\mathrm{R,min}}$ are saturating (logistic) functions of T:

$$\begin{aligned} N_{\mathrm{S,max}}(T) &= p_{1,\mathrm{max}}/(1+e^{-p_{2,\mathrm{max}}(T-p_{3,\mathrm{max}})})+p_{4,\mathrm{max}}\ , \\ N_{\mathrm{R,min}}(T) &= p_{1,\mathrm{min}}/(1+e^{-p_{2,\mathrm{min}}(T-p_{3,\mathrm{min}})})+p_{4,\mathrm{min}}\ , \end{aligned} \tag{1}$$

where two shape parameters, a mid-point location parameter p_3 and a mid-point slope parameter p_2, as well as a scaling parameter p_1 depend on the value of the initial inoculum, whereas an offset parameter p_4 almost does not change (see Supplementary Table 3). In particular, as follows from Supplementary Table 3, with increasing population density a scaling parameter's value (p_1) increases for both curves, whereas a mid-point location parameter's value (p_3) decreases. This implies that sensitive species prevail at a wider range of initial nutrient concentrations for higher population sizes. An offset parameter's value (p_4) is kept approximately at the same level for all initial population densities as well as a mid-point slope parameter's value (p_2) for the populations of low and intermediate sizes. The latter, however, changes dramatically at very high population sizes, which implies that the system reaches a saturation level faster for bigger populations.

For intermediate nutrient concentrations (between $N_{\mathrm{max,S}}$ and $N_{\mathrm{min,R}}$) the system exhibits frequency-dependent bistability whereby either S or R can outcompete each other. The size of the bistable region depends on the initial nutrient concentration as well as on the season length T as shown in Supplementary Fig 2. In addition, for a given T, increasing initial population density will result in an increase in the range of initial nutrient concentrations which support bistable dynamics. This is observed by noting that for a given T, $(N_{\mathrm{min,R}}-N_{\mathrm{max,S}})$ increases as the initial density increases.

Supplementary Table 3: Parameters values of Eq (1)

Parameters for the function $N_{\mathbf{S,max}}(T)$				
Initial inoculum	$p_{1,\max}$	$p_{2,\max}$	$p_{3,\max}$	$p_{4,\max}$
10^4 cells/ml	0.144512	0.285128	44.1068	1.17486
10^6 cells/ml	0.294247	0.281676	21.8297	1.17894
10^7 cells/ml	0.501968	0.328783	11.39	1.17523
Parameters for the function $N_{\mathbf{R,min}}(T)$				
Initial inoculum	$p_{1,\min}$	$p_{2,\min}$	$p_{3,\min}$	$p_{4,\min}$
10^4 cells/ml	0.146909	0.271046	42.1122	1.17393
10^6 cells/ml	0.297755	0.295111	19.5763	1.17967
10^7 cells/ml	0.5217	0.361761	9.48293	1.17271

3 Competition in the presence of drug

Please see Supplementary Figs 4 and 5.

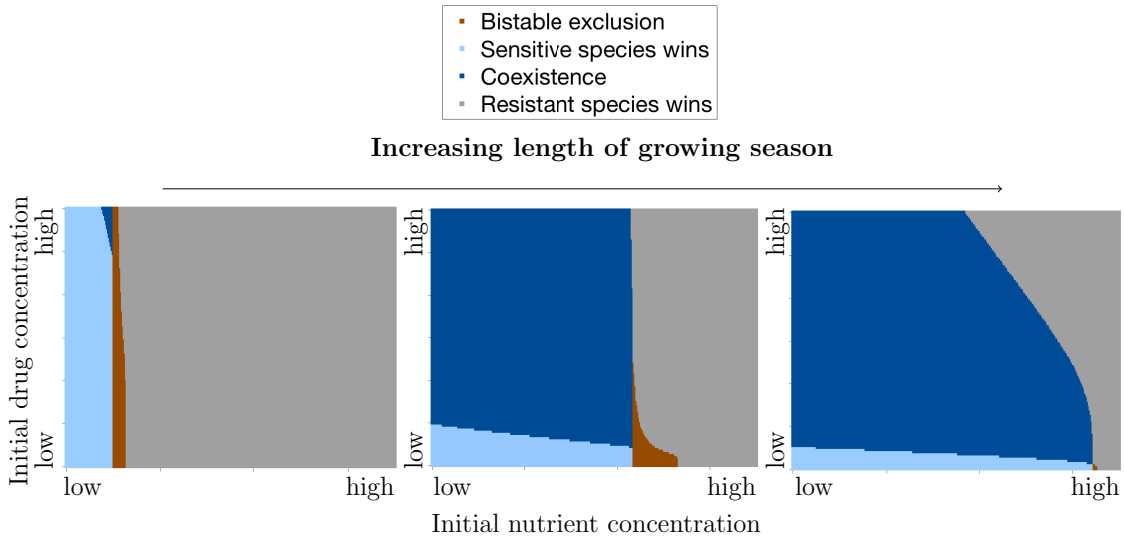

Supplementary Figure 4: Competition in the presence of drug. Theoretical two-dimensional dose-response mosaics describing the outcomes of competition between sensitive and resistant species at varying initial nutrient and drug concentrations within one growing season of three different lengths increasing from left to right. Results are obtained by means of simulations of the model (5) from the main text with the parameters values taken from Supplementary Table 1 and the initial community density fixed at 10^6 cells/ml value. Each axis corresponding to the initial nutrient concentration is plotted from 1.15% to 1.5% glucose, and each axis corresponding to the initial drug concentration is plotted from 0 μg/ml to 12 μg/ml fluconazole.

4 Competition in a chemostat environment

We also investigate the behaviour of the system in a chemostat environment by changing the model (5) from the main text the following way:

$$
\begin{cases}
\dot{N}(t) = d \times (N_0 - N(t)) - q_{\mathrm{S}}(N(t)) \times X_{\mathrm{S}}(t) - q_{\mathrm{R}}(N(t)) \times X_{\mathrm{R}}(t) \\
\dot{D}_{\mathrm{ex}}(t) = d \times (D_{\mathrm{ex},0} - D_{\mathrm{ex}}(t)) + (E(D_{\mathrm{in,S}}(t)) - I(D_{\mathrm{ex}}(t))) \times X_{\mathrm{S}}(t) \\
+ (E(D_{\mathrm{in,R}}(t)) - I(D_{\mathrm{ex}}(t))) \times X_{\mathrm{R}}(t) \\
\dot{D}_{\mathrm{in,S}}(t) = (I(D_{\mathrm{ex}}(t)) - E(D_{\mathrm{in,S}}(t))) \times X_{\mathrm{S}}(t) \qquad t \in [0,T] \\
\dot{D}_{\mathrm{in,R}}(t) = (I(D_{\mathrm{ex}}(t)) - E(D_{\mathrm{in,R}}(t))) \times X_{\mathrm{R}}(t) \\
\dot{X}_{\mathrm{S}}(t) = G_{\mathrm{S}} \times q_{\mathrm{S}}(N(t)) \times n_{\mathrm{ATP,S}} \times X_{\mathrm{S}}(t) \times i(D_{\mathrm{in,S}}(t)) - d \times X_{\mathrm{S}}(t) \\
\dot{X}_{\mathrm{R}}(t) = G_{\mathrm{R}} \times q_{\mathrm{R}}(N(t)) \times n_{\mathrm{ATP,R}} \times X_{\mathrm{R}}(t) - d \times X_{\mathrm{R}}(t)
\end{cases}
\tag{2}
$$

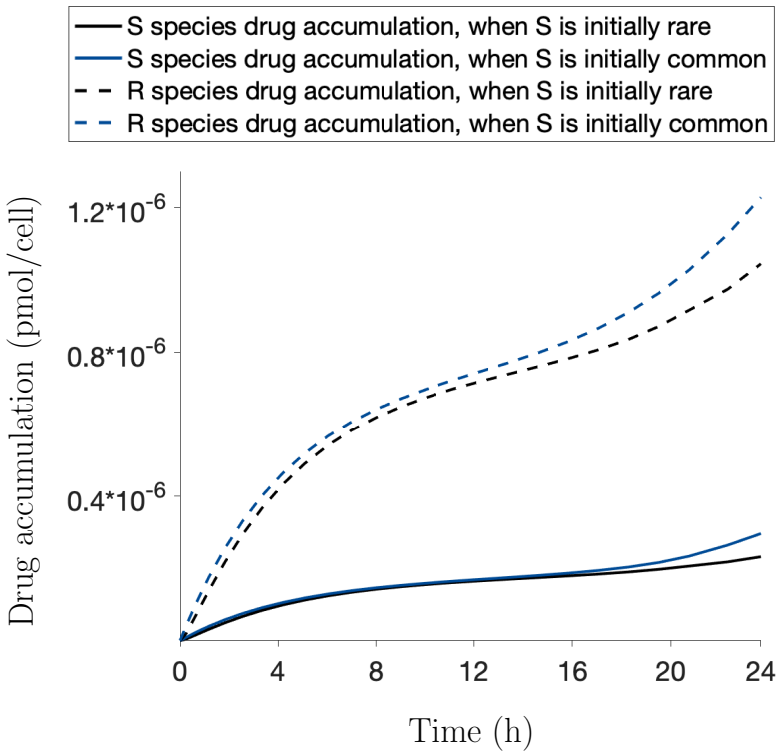

Supplementary Figure 5: Intracellular fluconazole accumulation (pmol/cell) for *C. albicans* (solid curve) and *C. glabrata* (dashed curve) in competition over 24 h in an initial glucose concentration of 1.3% and 2 μg/ml fluconazole (conditions where coexistence is predicted by the model (5) from the main text). Results are obtained by simulating the model (5) from the main text with parameter values from Supplementary Table 1 and an initial density of 10^6 cell/ml.

Here, the dynamics of competition between S and R within a single season of a length T begins with the introduction of the drug $D_{\mathrm{ex},0}$ and the limiting nutrient N_0 from the reservoir into the culture with the dilution rate d while observing the densities of both species X_{S} and X_{R} in the culture. All other state variables and parameters as well as axillary functions have a biological interpretation and a mathematical form as in the model (5) in the main text. We further define an environmental disturbance in a chemostat as a mass mortality, so that a disturbance to resource and drug concentrations is not manually introduced. Supplementary Fig 6 shows very similar patterns of competition outcomes to batch culture (cf. Fig 2 in the main text), albeit across slightly different timescales.

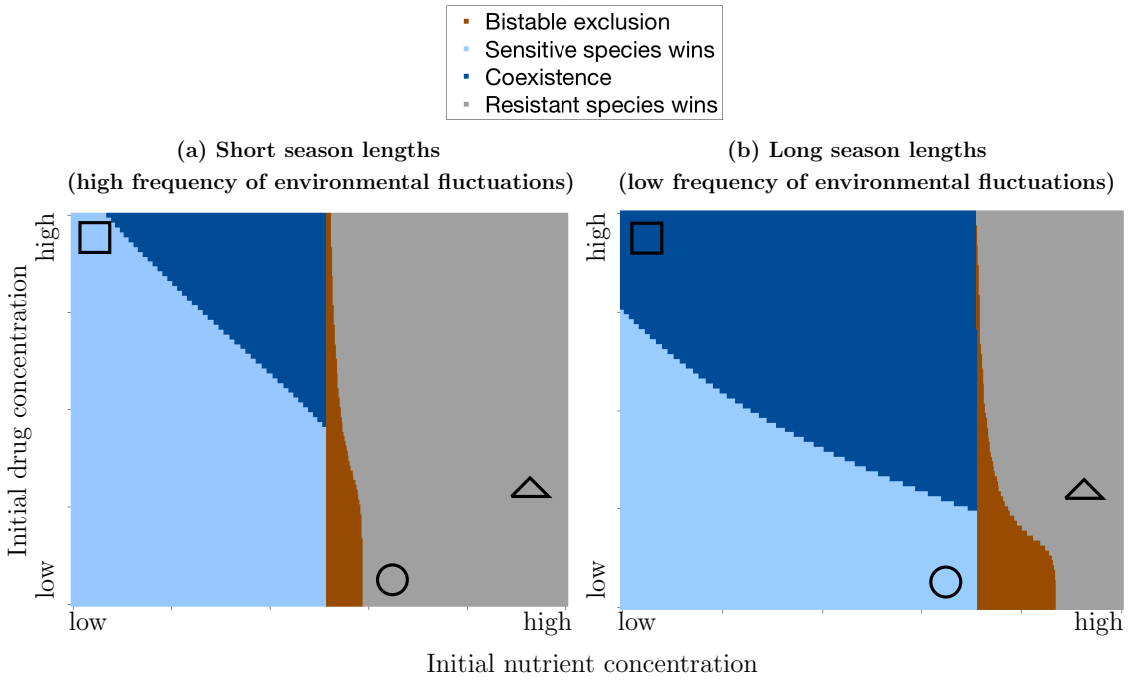

Supplementary Figure 6: Theoretical two-dimensional dose-response mosaics describing the equilibrium outcomes of competition in a chemostat environment between sensitive and resistant species at varying initial nutrient and drug concentrations within one growing season of two different lengths: (a) short, corresponding to the high frequency of environmental disturbance, (b) and long, corresponding to the low frequency of environmental disturbance. Results are obtained by means of simulations of the model (2) from the supplementary text with the parameters values taken from Supplementary Table 1 and the initial community density fixed at 10^6 cells/ml value. The dilution rate of a chemostat is fixed at 0.0017 per min, which is taken from an experimental study of competition in a chemostat for glucose between *Saccharomyces cerevisiae* and *Candida utilis* that are similar microbes in terms of their physiology and metabolism to *Candida glabrata* and *Candida albicans*, respectively [7]. Each axis corresponding to the initial nutrient concentration is plotted from 1% to 1.5% glucose, and each axis corresponding to the initial drug concentration is plotted from 0 μg/ml to 0.4 μg/ml fluconazole.

5 Flow cytometry

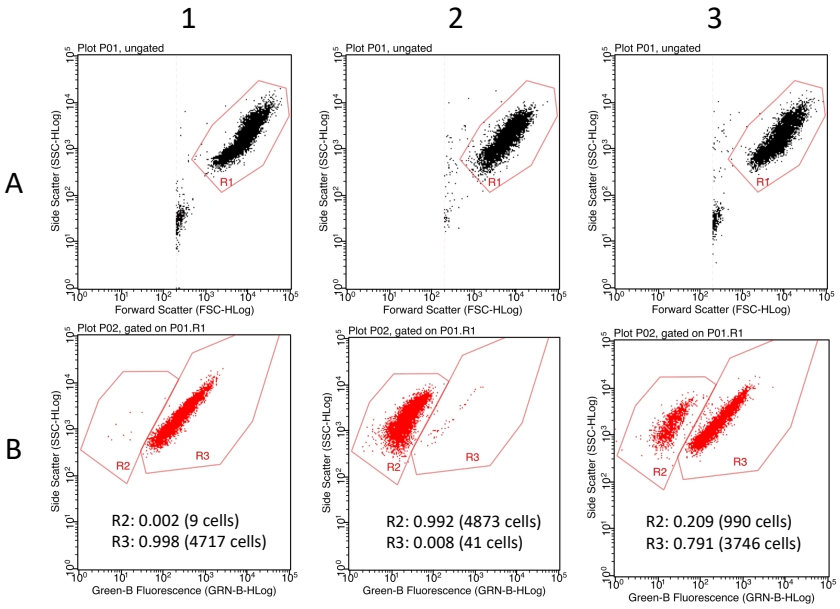

Supplementary Figure 7: Flow cytometry. Cells were distinguished as *C. albicans* or *C. glabrata* using flow cytometry based on differing green fluorescent protein expression. Row A shows events plotted as Forward scatter (FSC) against Side Scatter (SSC) for samples containing (1) *C. albicans* only, (2) *C. glabrata* only, or (3) a mixture of the two species. Events were gated based on FSC and SSC plots (R1) and then plotted as GFP intensity against SSC to separate the strains (Row B). Gates R2 for *C. albicans* and R3 for *C. glabrata* are based on the analysis of axenic cultures such that there is a false positive detection rate within the gated region of < 3 %. Plots shown were generated using Guava InCyte software (Merck Millipore).

References

[1] Pfeiffer T, Morley A. An evolutionary perspective on the Crabtree effect. Front Mol Biosci. 2014;1(17):1–6.

[2] van Urk H, Postma E, Scheffers WA, van Dijken JP. Glucose Transport in Crabtree-positive and Crabtree-negative Yeasts. J Gen Microbiol. 1989;135(9):2399–2406.

[3] Aquilla T. The Biochemistry of Yeast: Debunking the Myth of Yeast Respiration and Putting Oxygen in its Proper Place. Brewing Techniques. 2013;5(2).

[4] Hagman A, Säll T, Compagno C, Piskur J. Yeast "Make-Accumulate-Consume" Life Strategy Evolved as a Multi-Step Process That Predates the Whole Genome Duplication. PLoS ONE.

2013;8(7):e68734.

[5] Ray D, Goswami R, Banerjee U, Dadhwal V, Goswami D, Mandal P, et al. Prevalence of *Candida glabrata* and its response to boric acid vaginal suppositories in comparison with oral fluconazole in patients with diabetes and vulvovaginal candidiasis. Diabetes Care. 2007;30(2):312–317.

[6] Fidel PLJ, Vazquez JA, Sobel JD. *Candida glabrata*: review of epidemiology, pathogenesis, and clinical disease with comparison to *C. albicans*. Clin Microbiol Rev. 1999;12(1):80–96.

[7] Postma E, Kuiper A, Tomasouw WF, Scheffers WA, van Dijken JP. Competition for Glucose between the Yeasts *Saccharomyces cerevisiae* and *Candida utilis*. Appl Environ Microbiol. 1989;55(12):3214–3220.

[8] Ene IV, Brunke S, Brown AJP, Hube B. Metabolism in Fungal Pathogenesis. Cold Spring Harb Perspect Med. 2014;4(12):a019695.

[9] Beardmore RE, Cook E, Nilsson S, Smith AR, Tillmann A, Esquivel BD, et al. Drug-mediated metabolic tipping between antibiotic resistant states in a mixed-species community. Nat Ecol Evol. 2018;2:1312–1320.